

polyamine toxins (Eldefrawi et al., 1988), peptide neurotoxins (Yasuhara et al., 1987; Konno et al., 1998) and a protein paralyzing toxin (Yamamoto et al., 2007) have so far been found in several solitary wasp venoms. Besides the neurotoxins, we have found that cytolytic peptides are also present in the solitary wasp venoms. Eumenine mastoparan-AF (EMP-AF) was the first to be found (Konno et al., 2000; dos Santos Cabrera et al., 2004), having similar characteristics to those of mastoparan, a representative of the cytolytic peptides in social wasp venoms. Eumenitin is also homologous to mastoparan, but has an extra hydrophilic amino acid at the C-terminus without amide modification (Konno et al., 2006). Anoplin was isolated from spider wasp venom and is the smallest molecule in this type of peptides (Konno et al., 2001). Decoralin, another linear cationic α -helical peptide, has features similar to anoplin, but like EMP-AF vs. eumenitin, it has an extra hydrophilic amino acid without amide modification at the C-terminus (Konno et al., 2007). Except for anoplin, these cytolytic peptides were found in solitary eumenine wasps, alternatively called “mud dauber wasps” or “potter wasps”, because they construct their pot-shaped nest with mud. Additionally, the eumenine wasps prey only on caterpillars, Lepidopteron larvae.

In our continuing survey of biologically active substances in solitary wasp venoms, we have isolated four new linear cationic α -helical peptides from two species of the eumenine solitary wasps, *Eumenes rubrofemoratus* and *Eumenes fraterculus*. Two of them, named eumenitin-R and eumenitin-F, are highly homologous to eumenitin, whereas the other two, named eumenine mastoparan-ER (EMP-ER) and eumenine mastoparan-EF (EMP-EF), are similar to EMP-AF, and thus, can be classified as mastoparan peptides. We now report the isolation, chemical characterization and biological evaluation of these novel peptides, including a secondary structure analysis and pore-forming activity.

2. Materials and methods

2.1. Purification

Female wasps of *E. rubrofemoratus* and *E. fraterculus* were collected at Yokohama, Kanagawa in Japan. The collected specimens were immediately frozen by dry ice and kept at $-75\text{ }^{\circ}\text{C}$ until use. The venom sacs were dissected immediately after being thawed and then lyophilized.

Fourteen lyophilized venom sacs of *E. rubrofemoratus* were extracted ($5 \times 1\text{ mL}$) with 1:1 acetonitrile–water containing 0.1% TFA ($\text{CH}_3\text{CN}/\text{H}_2\text{O}/0.1\%$ TFA). The extract was lyophilized, re-dissolved in 50 μL of water and subjected to reversed-phase HPLC (Shimadzu Corp., Kyoto, Japan) using CAPCELL PAK C_{18} , $6 \times 150\text{ mm}$ (SHISEIDO Co., Ltd., Tokyo, Japan) with linear gradient from 5% to 65% $\text{CH}_3\text{CN}/\text{H}_2\text{O}/0.1\%$ TFA at a flow rate of 1 mL/min over 30 min (Fig. 1A) to give eumenitin-R and EMP-ER eluted at 26.1 and 27.6 min, respectively.

Twenty lyophilized venom sacs of *E. fraterculus* were subjected to the same extraction procedure to give eumenitin-F and EMP-EF eluted at 26.2 and 29.0 min, respectively (Fig. 1B).

2.2. Mass spectrometry

All mass spectra were acquired on an Autoflex TOF/TOF mass spectrometer (Bruker Daltonics, Yokohama, Japan) equipped with 337 nm pulsed nitrogen laser under reflector mode. The accelerating voltage was 20 kV. Matrix, α -cyano-4-hydroxycinnamic acid (Aldrich), was prepared at a concentration of 10 mg/mL in 1:1 $\text{CH}_3\text{CN}/0.1\%$ TFA. External calibration was performed with [Ile^7]-angiotensin III (m/z 897.51, monoisotopic, Sigma) and human ACTH fragment 18–39 (m/z 2465.19, monoisotopic, Sigma). The sample solution (0.5 μL) dropped onto the MALDI sample plate was added to the matrix solution (0.5 μL) and allowed to dry at room temperature.

For TOF/TOF measurement, argon was used as a collision gas and ion was accelerated at 19 kV. The series of b and y ions were obtained which enabled identification of whole amino acid sequence by manual analysis.

2.3. Amino acid sequencing

Automated Edman degradation was performed by a gas-phase protein sequencer PPSQ-10 (Shimadzu Corp., Kyoto, Japan).

2.4. Peptide synthesis

The peptides were synthesized using Fmoc chemistry on a Prelude peptide synthesizer (Protein Technologies, Tucson, AZ) at a scale of 20 μmol . The synthesis of the peptide amides involved a 1 h offline swell of the Rink Amide MBHA resin in dichloromethane at room temperature prior to online synthesis. The peptide acids were synthesized using pre-loaded Wang resin. Subsequent residues, at a concentration of 100 mM, were double coupled using 20% piperidine as the deprotector and 1H-Benzotriazolium 1-[bis(dimethylamino)methylene]-5chloro-, hexafluorophosphate (1),3-oxide (HCTU) as the activator.

Cleavage was performed online with 95:2.5:2.5 TFA:–water:triisopropylsilane. The cleaved peptides were removed from the synthesizer and their TFA volumes were reduced under a stream of nitrogen. Ice cold ether was added to precipitate the peptides and after centrifugation at 13,000 rpm for 5 min, the ether layer was poured off. The pellets were resolubilized in 0.1% TFA and lyophilized (Modulyod, Thermo Savant).

The lyophilized pellets were resolubilized in 4 mL 12.5% acetonitrile, 0.1% TFA in water. Purification was carried out by reversed-phase HPLC Ultimate 3000 (Dionex, Sunnyvale, CA), monitoring peptide elution at 230 nm. Approximately 20 mg of the crude peptides were chromatographed using an Onyx Monolithic C_{18} column ($10 \times 100\text{ mm}$, 13 nm & 2 μm pore size) with a linear gradient of 0.1% TFA in water (v/v) and 0.85% TFA in acetonitrile (v/v) at a flow rate of 5 mL/min over 25 min.

The fractions of interest were spotted onto a stainless steel MALDI plate and observed by MALDI-TOF (Applied Biosystems/MDS SCIEX, Foster City, CA). Fractions containing greater than 80% purity were pooled and lyophilized. The synthetic peptides were used in the assays below.

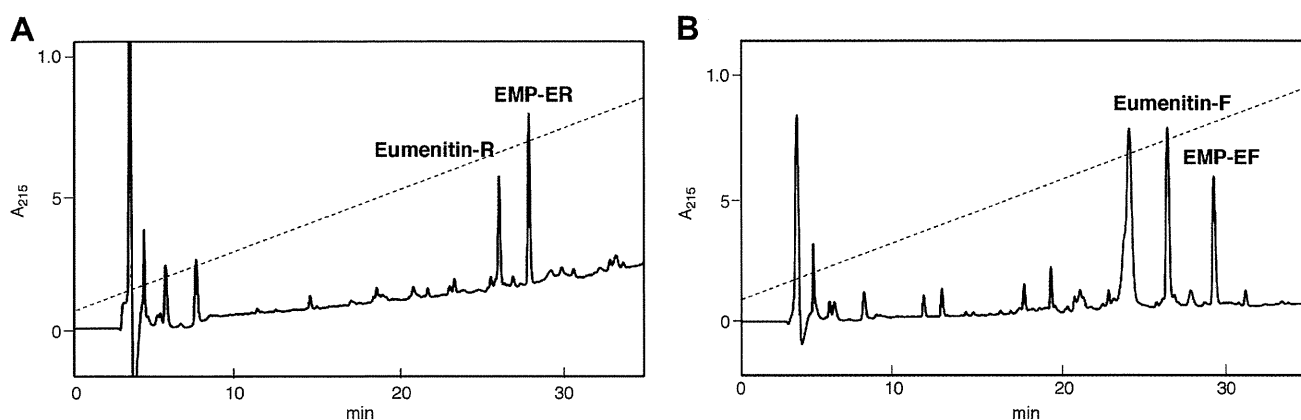


Fig. 1. Fractionation of venom extracts of (A) *Eumenes rubrofemoratus* and (B) *Eumenes fraternulus* by reverse-phase HPLC using CAPCELL PAK C₁₈ (6 × 150 mm) with linear gradient of 5–65% CH₃CN/H₂O/0.1% TFA over 30 min at flow rate of 1 mL/min. UV absorption was monitored at 215 nm.

2.5. Circular dichroism (CD) spectroscopy

2.5.1. Small vesicles preparation (SUV)

Chloroform solution of asolectin was evaporated under N₂ flow, rendering homogeneous films on round bottom flasks that were further dried under vacuum for at least 3 h. Films were hydrated at room temperature with buffer (Tris/H₃BO₃ 5 mM, 0.5 mM Na₂EDTA, 150 mM NaF, pH 7.5) to reach a final lipid concentration of 10 mg/mL and vortex mixed. SUVs were obtained after 50 min sonication (or until clear) with a tip sonicator in an ice/water bath, under N₂ flow; titanium debris was removed by centrifugation. SUVs were then submitted to 6 extrusions, at room temperature, through a 100 nm polycarbonate membrane followed by 11 extrusions through two stacked 50 nm polycarbonate membranes, using an Avanti mini-extruder. SUVs were kept under refrigeration and used in the same day of preparation.

2.5.2. CD spectroscopy experiments

CD spectra were obtained at 20 μM peptide concentration in different environments: bi-distilled water, 5 mM Tris/H₃BO₃ buffer, pH 7.5, 8 mM sodium dodecylsulfate (SDS) solution (above critical micelle concentration), 40% v/v trifluoroethanol (TFE)/water mixture, and in the presence of 100 and 250 μg/mL asolectin vesicles. TFE solutions are known inductors of helical structures and micellar SDS as well as vesicles are membrane mimetic environments with anionic character, a feature common to bacterial membranes (Yeaman and Yount, 2003). At 40% TFE or at micellar concentration of SDS solutions (8 mM) they tend to induce the maximum observable values (Prates et al., 2004). In the presence of asolectin vesicles saturation was found at 250 μg/mL concentration.

CD spectra were recorded from 260 to 203 or 190 nm (depending on signal-to-noise ratio) with a Jasco-710 spectropolarimeter (JASCO International Co. Ltd., Tokyo, Japan) which was routinely calibrated at 290.5 nm using *d*-10-camphorsulfonic acid solution. Spectra were acquired at 25 °C using 0.5-cm path length cell, averaged over eight scans, at a scan speed of 20 nm/min, bandwidth of 1.0 nm,

0.5 s response, and 0.2 nm resolution. Following baseline correction, the observed ellipticity, θ (mdeg), was converted to mean-residue ellipticity, $[\Theta]$ (deg cm²/dmol), using the relationship $[\Theta] = 100 \theta / (lc n)$ where 'l' is the path length in centimeters, 'c' is peptide millimolar concentration, and 'n' the number of peptidic bonds. Assuming a two state model, the observed mean-residue ellipticity at 222 nm ($[\Theta]_{222}^{obs}$) was converted into α -helix fraction (f_H) using the method proposed by Rohl and Baldwin (1998) and previously described (Konno et al., 2001).

2.6. Channel-like incorporation in mimetic lipid bilayers

2.6.1. Bilayer formation

The lipid bilayers were obtained from giant unilamellar vesicles (GUVs), which were positioned onto the chip aperture by application of negative pressure. The GUVs burst as soon as they touch the glass surface of the chip and form a bilayer that spans the aperture (Sondermann et al., 2006). Asolectin (Sigma), a negatively charged mixture of lipids, was used to form artificial membranes. GUVs were formed by electrosweeling, using the Nanion Technologies (Munich, Germany) device Vesicle Prep Pro®. 20 μL of 10 mg/mL lipid solution (in chloroform) were deposited onto an indium tin oxide (ITO) coated glass plate and evaporated for 45–60 min. A nitrile ring was placed around the dried lipid film and filled with 350 μL of 250 mM D-Sorbitol dissolved in Milli-Q water. A second ITO coated glass plate was placed on top of the ring. An AC voltage of 3 V peak-to-peak amplitude at 5 Hz frequency was supplied to the ITO slides over a period of 2 h at 36 °C (modified from Sondermann et al., 2006). The formed vesicles were kept in plastic vials under refrigeration (4 °C) until use or used immediately. GUVs suspensions were always observed under light microscope prior to use.

2.6.2. Electrophysiology

The experiments were performed with the automated Patch-Clamp device Port-a-Patch (Nanion Technologies – Munich, Germany), using borosilicate glass chips NPC-1 with aperture diameter of approximately 1 μm. The

resistance of the apertures was approximately 1–3 M Ω in 150 mM HCl solution. Current signals were amplified and recorded by an amplifier EPC-10 (Heka Elektronik, Lambrrecht, Germany) and an analogical/digital interface ITC-1600. The system was computer controlled by the PatchControl™ software (Nanion) (Fertig et al., 2002; Sondermann et al., 2006).

During the experiments symmetrical solution of 150 mM HCl with 5 mM Tris was used. After a seal was formed ($R_m > 500$ m Ω), the peptides diluted with Milli-Q water at a 5 μ M concentration were added to the *cis* side of the chip (top) to observe the single channel activity. The volume of peptide solution was never superior to 10% of the solution at the *cis* side. Voltage pulses were applied at the *trans* side of the chip (bottom). Usually, single channel activity started approximately 10 min after adding the peptides, as monitored by a constant V_{hold} of -100 mV. Single channel conductance of incorporated channels was determined under positive and negative voltage pulses. The experiments were performed at room temperature (~ 22 °C). The data was analyzed by PatchMaster and Matlab softwares.

2.7. Antimicrobial activity

The microorganisms used were: *Staphylococcus aureus* ATCC 25923, *Micrococcus luteus* ATCC 10240, *Staphylococcus epidermidis* (clinical sample), *Streptococcus pyogenes* (clinical sample), *Bacillus subtilis* ATCC 6633, *Escherichia coli* ATCC 25922, *Proteus mirabilis* (clinical sample), *Stenotrophomonas maltophilia* ATCC 13637, *Pseudomonas aeruginosa* ATCC 27853 and *Candida albicans* ATCC 90112.

The MICs of the tested peptides were determined by 2-fold serial broth microdilution in Müller–Hinton broth (Difco) in 96-well plates. Aliquots of 45 μ L of Müller–Hinton broth (Difco) were placed in the microplates containing 50 μ L of the peptides solutions. The mixture was completed by inoculation of 5 μ L of bacterial suspension (10^7 CFU/mL), according NCCLS (Wayne, 2004), resulting in a final volume of 100 μ L with 10^4 CFU/well. Following inoculation, the microtitre plates were incubated at 37 °C for 18 h before the results were recorded. After this time, the turbidity of the cultures was measured in an ELISA reader at 595 nm to assess bacterial growth. The results were expressed as inhibition percentage of optical density (OD) against a control; this control was obtained in each situation by measuring the OD of the microorganisms introduced into the plate in the absence of peptide. Also, the lowest concentration of peptide at which there is no visible growth after overnight incubation was observed.

2.8. Hemolytic activity

A 4% suspension of mouse erythrocytes (ES) was prepared as described (Rangel et al., 1997). Different concentrations of the peptides were incubated with the ES at room temperature (~ 22 °C) in an Elisa plate (96 wells). After 1 h it was centrifuged ($1085 \times g/5$ min), and the hemolytic activity of the supernatant was measured by the absorbance at 540 nm, considering as blank the absorbance of Krebs–Henseleit physiological solution (mM: NaCl 113;

KH₂PO₄ 1.2; KCl 4; MgSO₄ 1.2; CaCl₂ 2.5; NaHCO₃ 25; glucose 11.1), which was the vehicle for the peptides. Total hemolysis was obtained with 1% Triton X-100 and the percentage of hemolysis was calculated relative to this value.

2.9. Mast cell degranulation activity

The ability of the peptides to induce mast cells degranulation was investigated *in vitro* using the protocol of quantification of the granular enzyme β -hexosaminidase released in the supernatants of PT18 cells (a connective tissue-type mast cell model) and RBL-2H3 cells (a mucosal-type mast cell model), according to Ortega et al. (1991). For this, 4×10^6 PT18 cells or 1.2×10^5 RBL-2H3 cells (200 μ L) were incubated in the presence of the peptides for 30 min in Tyrode's buffer at 37 °C/5% CO₂. After this, the cells were centrifuged and the supernatants collected. The cells incubated only with the Tyrode's buffer were lysed with 0.5% Triton X-100 (200 μ L) (Sigma–Aldrich) solution to evaluate the total enzyme content. From each experimental sample to be assayed, four aliquots (10 μ L) of the supernatant were taken to separate microwell plates. To these samples, 90 μ L of the substrate solution containing 1.3 mg/mL of p-nitrophenyl-N-acetyl- β -D-glucosamine (Sigma) in 0.1 M citrate, pH 4.5, were added and the plates incubated for 12 h at 37 °C. The reactions were stopped by addition of 100 μ L of 0.2 M glycine solution, pH 10.7, and the optical density determined at 405 nm in an ELISA reader (Lab-systems Multiskan Ex). The extent of secretion was expressed as the net percentage of the total β -hexosaminidase activity in the supernatant of unstimulated cells. The results represent the mean of quadruplicate tests \pm standard deviation (SD).

2.10. Leishmanicidal activity

Medium 199 was used for the cultivation of promastigotes of *Leishmania major* (MHOM/SU/73/5ASKH). Promastigotes were cultured in the medium [supplemented with heat-inactivated (56 °C for 30 min) fetal bovine serum (10%)] at 27 °C, in a 5% CO₂ atmosphere in an incubator (Takahashi et al., 2004).

The leishmanicidal effects of the peptides were assessed using the improved 3-[4,5-dimethylthiazol-2-yl]-2,5-diphenyltetrasodium bromide (MTT) method as follows. Cultured promastigotes were seeded at $4 \times 10^5/50$ mL of the medium per well in 96-well microplates, and then 50 mL of different concentrations of test compounds dissolved in a mixture of DMSO and the medium were added to each well. Each concentration was tested in triplicate. The microplate was incubated at 27 °C in 5% CO₂ for 48 h. TetraColor ONE (10 mL) a mixture of 2-(2-methoxy-4-nitrophenyl)-3-(4-nitrophenyl)-5-(2,4-disulfophenyl)-2H-tetrazolium, monosodium salt and 1-methoxy-5-methylphenazinium methosulfate was added to each well and the plates were incubated at 27 °C for 6 h. Optical density values (test wavelength 450 nm; reference wavelength 630 nm) were measured using a microplate reader (Thermo BioAnalysis Japan Co., Ltd., Kanagawa, Japan). The values of 50% inhibitory concentration of the peptides were estimated from the dose–response curve.

Eumenitin	LNLKGIFKVASLLT
Eumenitin-R	LNLKGLIKKVASLLN
Eumenitin-F	LNLKGLFKKVASLLT
EMP-ER	FDIMGLIKKVAGAL-NH₂
EMP-EF	FDVMGIKKIASAL-NH₂
EMP-AF	INLLKIAKGIIKSL-NH₂
HR-1	INLKAIAALVKKVL-NH₂

Fig. 2. Amino acid sequences of the venom peptides from solitary eumenine wasp and HR-1 (Histamine Releasing peptide) from social wasp *Vespa orientalis* venom. Polar, charged residues are shown in bold types.

3. Results

3.1. Purification and sequence determination

The venom extracts of *E. rubrofemoratus* were subjected to reversed-phase HPLC, and the purity and complexity of each fraction was examined by MALDI-TOF MS. The HPLC profile was rather simple, having only several intense peaks (Fig. 1A). The two major fractions eluted at 26.1 and 27.6 min showed a high purity with protonated molecular ion peaks at m/z 1623.9 and 1474.9 (MH^+ , monoisotopic),

respectively. The molecular weight and chromatographic behavior suggested these components to be peptides, which we named eumenitin-R and eumenine mastoparan-ER (EMP-ER), respectively.

The sequence of the peptides was analyzed first by MALDI-TOF/TOF MS. Eumenitin-R had a sequence of 15 amino acids as I/L-N-I/L-K/Q-G-I/L-I/L-K/Q-K/Q-V-A-S-I/L-I/L-N, which was consistent with the observed molecular mass. However, contrary to expectation, there was no *d* or *w* ions observed, and therefore, no information about the I/L and K/Q differentiation. Accordingly, the sequence was determined by Edman degradation using an automated sequencer, giving whole sequence as L-N-L-K-G-L-I-K-K-V-A-S-L-L-N. The solid-phase synthesis of this peptide and the HPLC comparison of the synthetic specimen with the natural peptide finally corroborated the sequence.

The MALDI-TOF/TOF MS analysis of EMP-ER showed a 14 amino acid sequence with a C-terminal amide as F-D-I/L-M-G-I/L-I/L-K/Q-K/Q-V-A-G-A-I/L-NH₂, which was consistent with the observed molecular mass. However, there was again no information about the I/L differentiation. Edman degradation suggested a 13 amino acid sequence as F-D-I-M-G-L-I-K-K-V-A-G-A, and so, the C-terminal I/L was still

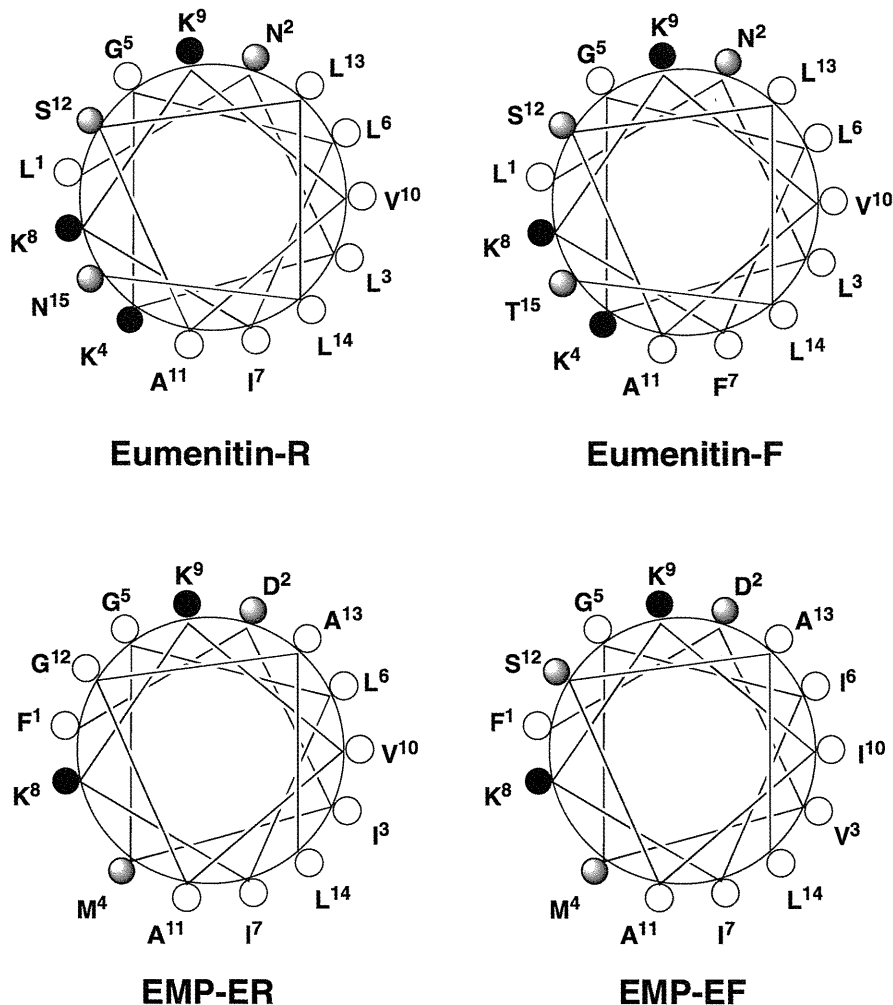


Fig. 3. Helical wheel projection of the sequences of the novel wasp venom peptides. In this view through the helix axis, the hydrophilic Ser (S), Thr (T), Asn (N) and Lys (K) residues are located on one side and the hydrophobic Ile (I), Leu (L) and Val (V) residues on the other side of the helix.

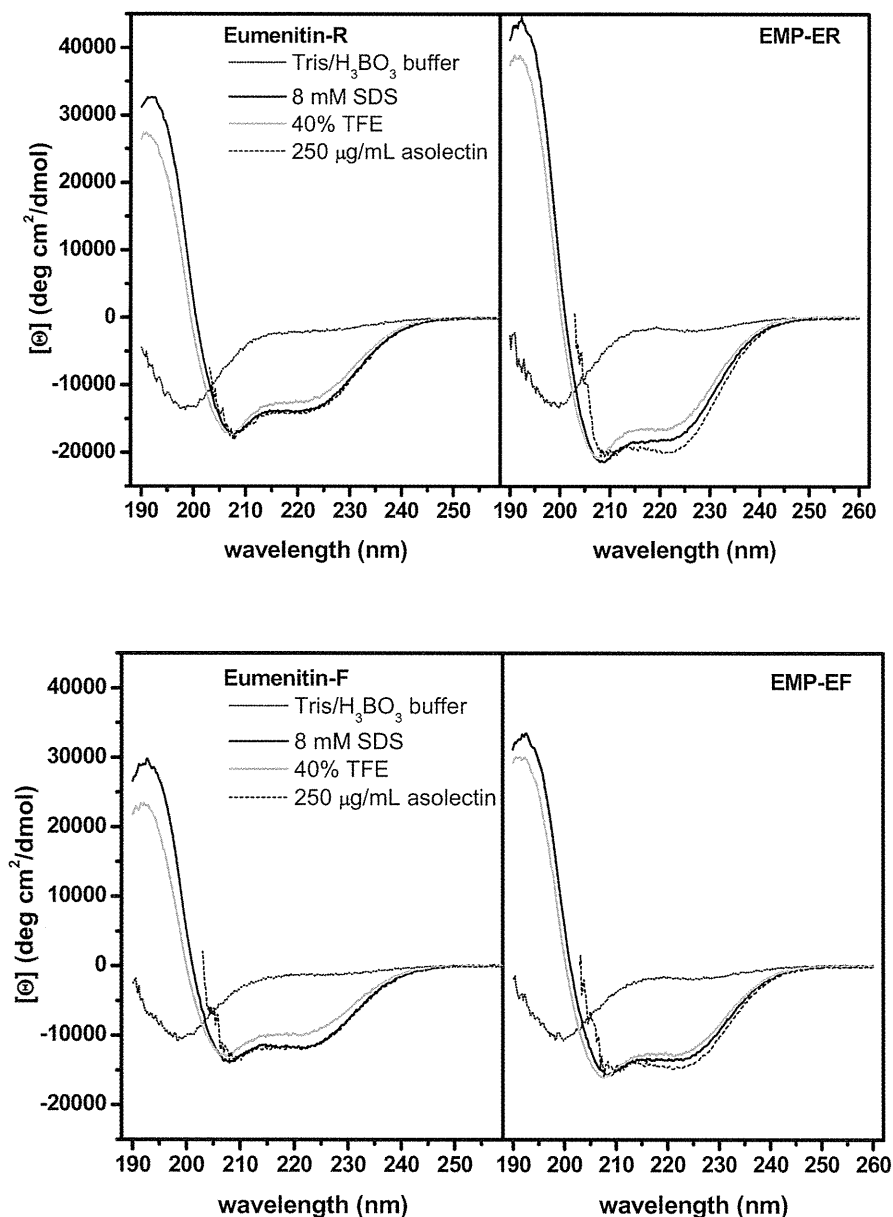


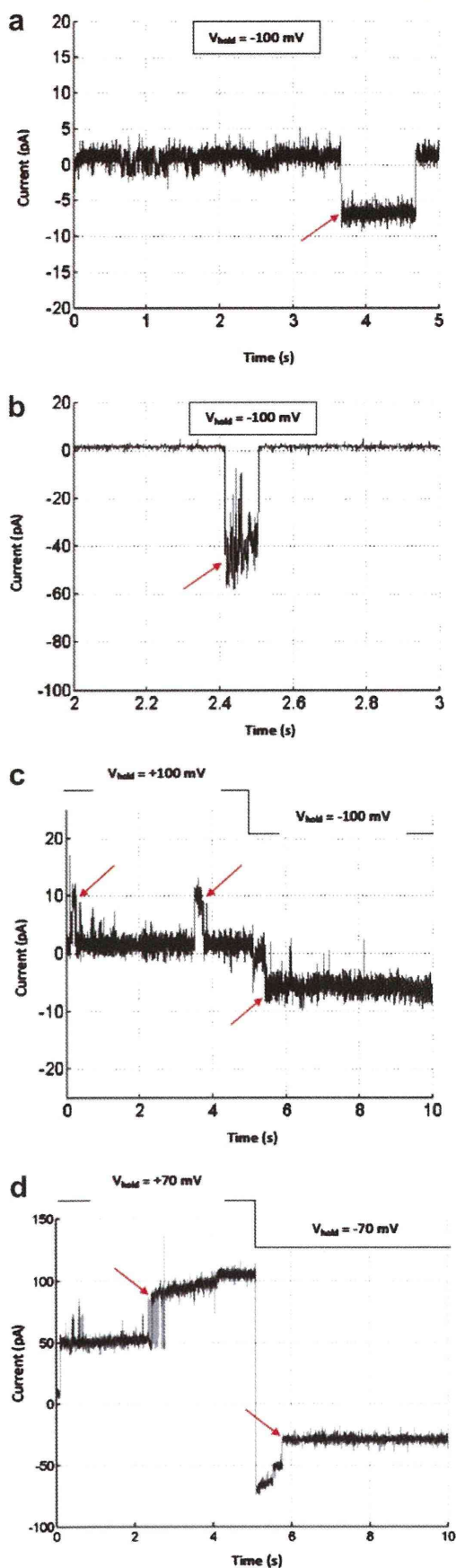
Fig. 4. CD spectra of the four peptides, eumenitin-R, EMP-ER, eumenitin-F and EMP-EF, obtained at 20 μM peptide concentration, at 25 $^{\circ}\text{C}$ in different environments. Peptides assume an α -helical conformation in 40% TFE, 8 mM SDS and in the presence of asolectin vesicles, showing modest preference for the anionic environments of SDS micelles and asolectin vesicles.

not determined. Finally, it was determined by the solid-phase synthesis of both the ^{14}I and ^{14}L peptides and their HPLC behavior was compared to the natural peptide. As a consequence, the ^{14}L peptide was found to be identical to the natural one, and therefore, the sequence was unambiguously determined as F-D-I-M-G-L-I-K-K-V-A-G-A-L-NH₂.

Similarly, eumenitin-F and eumenine mastoparan-EF (EMP-EF) were purified from the extracts of *E. fraterculus* (Fig. 1B), and in the same manner, the sequences were determined to be L-N-L-K-G-L-F-K-K-V-A-S-L-L-T and F-D-V-M-G-I-I-K-K-I-A-S-A-L-NH₂, respectively. The chemical features of these new peptides, rich in hydrophobic and basic amino acids with no disulfide bond, are characteristic of linear cationic cytolytic peptides (Kuhn-Nentwig, 2003),

in particular, eumenitin-R and eumenitin-F, are highly homologous to eumenitin, whereas the other two, EMP-ER and EMP-EF, are similar to EMP-AF, thus can be classified as mastoparans (Fig. 2, Murata et al., 2009). This class of peptides has been known to adopt an amphipathic α -helical conformation, showing an amphiphilic character under appropriate conditions (Wakamatsu et al., 1992; Hori et al., 2001; Sforça et al., 2004; Todokoro et al., 2006).

The amphipathicity of peptides has been considered essential for their biological activities (Wimley, 2010). In fact, if the helical wheel projections of these peptide sequences were drawn, they show that amphipathic α -helical conformations could be possible as depicted in Fig. 3. Based on this view, all the hydrophilic amino acid residues, S, T, N and K, are located on one side, whereas the



hydrophobic amino acid residues, I, L and V are on the other side of the helix.

3.2. CD spectroscopy

The Eumenine wasp venom peptides as well as mastoparan peptides are known to undergo a conformational change from a random coil to helical upon binding to lipid bilayers or in membrane mimetic environments (Park et al., 1995; dos Santos Cabrera et al., 2004; Konno et al., 2006). The α -helix content of these short chain peptides is directly related to favorable electrostatic interactions and the burial of the backbone into a more hydrophobic region. Fig. 4 shows the CD spectra of eumenitin-R, eumenitin-F, EMP-ER and EMP-EF obtained in different environments, to evaluate the relative importance of the electrostatic and hydrophobic contributions to the observed ellipticity. In water (spectra not shown) or in Tris/H₃BO₃ buffer, the spectra of the four peptides are equally characteristic of unordered structures, while assuming the features of an α -helical conformation with double minima around 208 and 222 nm in the membrane mimetic environments and in the presence of anionic asolectin vesicles (Fig. 4). The spectra acquired with 100 (not shown) and 250 μ g/mL lipid contents, to check for further binding, showed a slight increase in the helical content (f_H), which for the four peptides is favored in the presence of anionic environments such as an 8 mM SDS solution or asolectin vesicles as already observed with EMP-AF (dos Santos Cabrera et al., 2004), eumenitin (Konno et al., 2006) and decoralin (Konno et al., 2007). These findings indicate that these helical peptides may present an amphipatic structure as determined for EMP-AF (Sforça et al., 2004) and mastoparans (Wakamatsu et al., 1992; Chuang et al., 1996; Hori et al., 2001; Todokoro et al., 2006).

3.3. Channel-like incorporation in mimetic lipid bilayers

The novel wasp venom peptides, at concentrations of 0.5–2 μ M, induced an ion channel-like incorporation in lipid bilayers formed from the GUVs of asolectin (Figs. 5 and 6) under positive and negative voltage pulses, using a 150 mM HCl solution, within a 10 min incubation time. At peptide concentrations higher than 2 μ M, the great number of incorporated channels (over 10) induced a breakdown of the lipid bilayers 2–3 s after applying our standard initial V_{hold} of -100 mV. The unitary channel conductances were determined at V_{hold} of $+100$ and -100 mV (see Table 2). Different levels were detected in different peptide sequences (Figs. 5 and 6), and only eumenitin-F and -R formed pores with conductances higher than 500 pS. From that we can assume that clusters can be formed and several units of the peptides organize to form bigger pores. Rectification was detected only in the eumenitin-F channels. Similar ion-channel like activity

Fig. 5. Single channel incorporation in asolectin lipid bilayers in the presence of the peptides eumenitin-R (a and b) and eumenitin-F (c and d) (0.5–2 μ M). Solution: 150 mM HCl (symmetrical). Arrows indicate some channel apertures/closings. (a) Conductance 80 pS; (b) conductance = 410 pS; (c) the conductances were 81 pS ($+100$ mV), and 73 pS (-100 mV); (d) conductances were 190 and 885.7 pS (70 mV), and 238.6 and 332.9 pS (-70 mV).

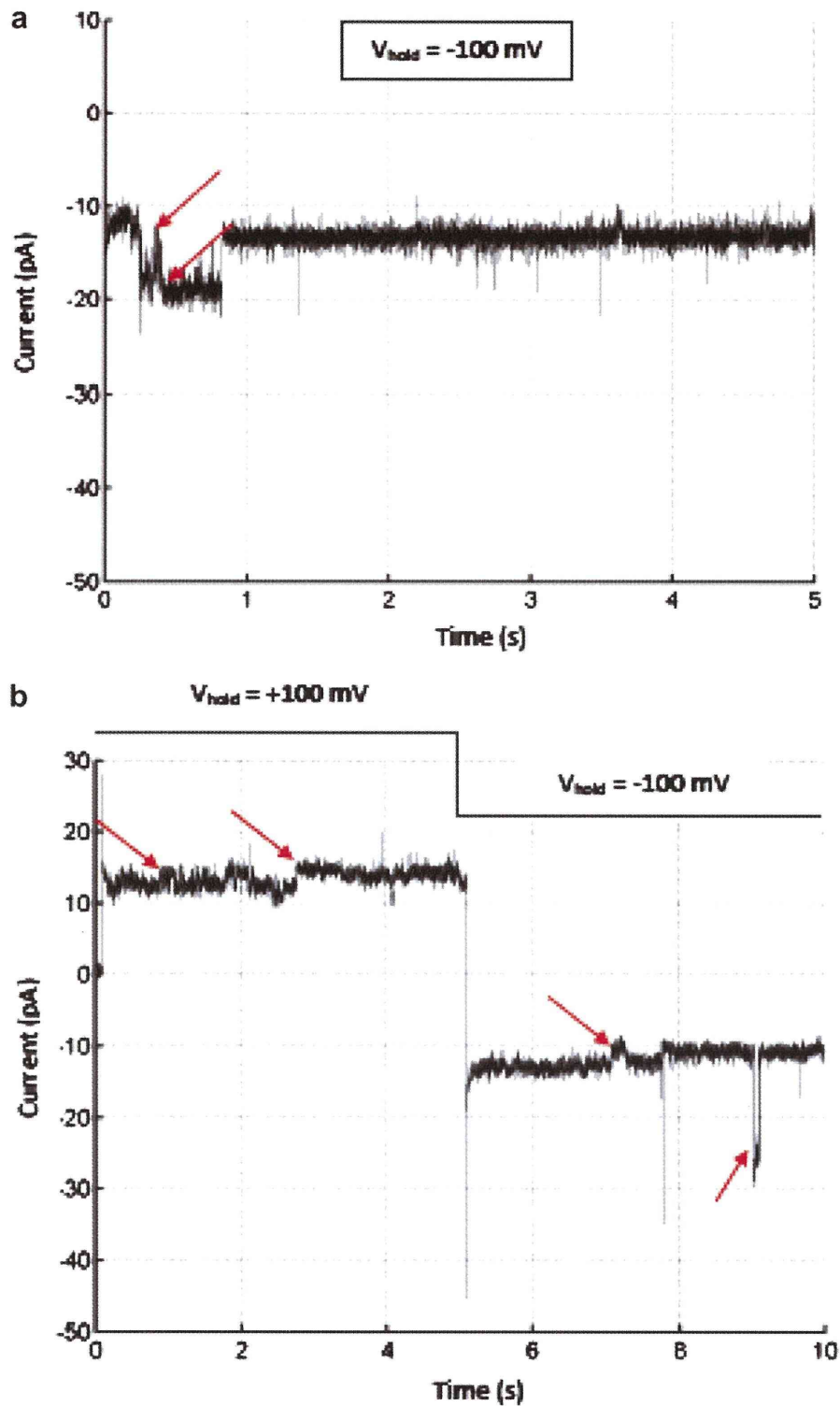


Fig. 6. Single channel incorporation in asolectin lipid bilayers in the presence of the peptides EMP-ER (a) and EMP-EF (b) (0.5–2 μ M). Solution: 150 mM HCl (symmetrical). Arrows indicate some channel apertures. (a) Conductances were 28 and 60 pS; (b) conductances were 35 and 60 pS (+100 mV) and 35 and 75 pS (–100 mV).

was found with other peptides from solitary and social wasp venoms, as anoplin (dos Santos Cabrera et al., 2008), eumenitin (Arcisio-Miranda et al., 2008) and HR-1 (dos Santos Cabrera et al., 2009), as discussed below.

3.4. Biological activities

The mast cell degranulation, hemolysis, antimicrobial and antiprotozoan (leishmanicidal) activities were tested

Table 1

Structural and physicochemical properties of the new wasp venom peptides in comparison to eumenitin and mastoparan HR-1. Features shown are: number of amino acid residues in the sequence (N_{aa}), net charge (Q), hydrophobicity (H), time elapsed in the HPLC elution process, in minutes, and α -helix fraction (standard deviation \pm 0.02).

	N_{aa}	Q ^a	H ^b	Elution time (min)	α -helix fraction		
					40% TFE	8 mM SDS	Asolectin
Eumenitin-R	15	+3	-0.034	26.1	0.43	0.48	0.49
EMP-ER	14	+2	0.131	27.6	0.53	0.59	0.65
Eumenitin-F	15	+3	-0.011	26.2	0.34	0.41	0.41
EMP-EF	14	+2	0.115	29.0	0.41	0.44	0.48
Eumenitin ^c	15	+3	0.002	Na	0.43	0.50 ^c	na
Mast. HR1 ^d	14	+4	0.067	Na	0.56	0.53	na

rc = random coil; na = unavailable.

^a For peptides with an amidated C-terminus, includes an extra-charge.

^b Calculated according to Eisenberg et al., consensus scale (1984).

^c Konno et al., 2006.

^d dos Santos Cabrera et al., 2009.

because these are characteristic biological activities for these types of peptide.

3.4.1. Antimicrobial activity

The peptide eumenitin-R was the most efficient in the antimicrobial assay, presenting the lowest MIC values against both Gram-positive and Gram-negative strains. Furthermore, all the peptides had more potent activities against the yeast *C. albicans* (Table 3). The four peptides described here showed an antimicrobial activity at very similar doses when compared to eumenitin (Konno et al., 2006).

3.4.2. Hemolytic activity

The solitary wasp peptides presented low to moderate hemolytic activities against mice erythrocytes in a dose-dependent manner (Fig. 7). A one-way analysis of variance (ANOVA) of the log EC₅₀ (50% effective concentration) followed by the Newman–Keuls multiple comparison test indicated that EMP-ER and EMP-EF were more effective than eumenitin-R and eumenitin-F in this assay, presenting lower EC₅₀ values (see Table 4 for EC₅₀ values). Generally speaking, these peptides can be considered weakly hemolytic, especially eumenitin-R. These results well correlated with the hydrophobicity and shorter elution times of the

Table 2

Mean, minimum and maximum conductances of anionic (AZO) bilayers induced by eumenine peptides according to the V_{hold} (3 different experiments).

Peptide	V_{hold} (mV)	Conductance (pS)	SEM	Minimum conductance (pS)	Maximum conductance (pS)
Eumenitin-R	-100	82.5	17.1	22	500
	+100	118.8	44	22	751
Eumenitin-F	-100	298.6	51	37	980
	+100	187.1	67.7	49	710
EMP-ER	-100	68.2	4	21	210
	+100	61.4	3.7	22	126
EMP-EF	-100	33.6	8.9	10	138
	+100	32.2	6.9	16	157

Table 3

Minimum inhibitory concentration (MIC) of the peptides from the wasps *Eumenes rubrofemoratus* (Eumenitin-R and EMP-ER) and *Eumenes fraternus* (Eumenitin-F and EMP-EF), in μ M.

Microorganism	Eumenitin-R	EMP-ER	Eumenitin-F	EMP-EF
Gram-positive				
<i>Staphylococcus aureus</i> ATCC 25923	60	30	>60	30
<i>Staphylococcus epidermidis</i> (clinical sample)	30	30	30	30
<i>Micrococcus luteus</i> ATCC 10240	15	>30	30	30
<i>Streptococcus pyogenes</i> (clinical sample)	15	>30	30	>30
<i>Bacillus subtilis</i> ATCC 6633	7.5	30	30	30
Gram-negative				
<i>Escherichia coli</i> ATCC 25922	30	30	30	30
<i>Proteus mirabilis</i> (clinical sample)	60	60	>60	60
<i>Pseudomonas aeruginosa</i> ATCC 27853	30	>30	30	>30
<i>Stenotrophomonas maltophilia</i> ATCC 13637	15	>30	15	>30
Yeast				
<i>C. albicans</i> ATCC 90112	<7.5	7.5	7.5	7.5

respective peptides (see Table 1). The erythrocytes membranes show a zwitterionic character (Yeaman and Yount, 2003), and peptides with a lower charge and higher hydrophobicity present a stronger interaction with this type of membrane (de Souza et al., 2010).

3.4.3. Mast cell degranulation

The ability of the peptides to induce mast cells degranulation was assayed *in vitro* in PT18 cells and RBL-2H3 cells, by the measurement of the enzyme β -hexosaminidase released. As shown in Fig. 8A, all the new peptides were able to induce mild degranulation in connective tissue-type mast cells with equivalent potencies and dose-dependent, similarly to Eumenitin, and weaker than mastoparan (Konno et al., 2006). On the other hand, in mucosal-type mast cells EMP-ER and EMP-EF, which are similar to EMP-AF, exhibited more intense mast cell degranulation than eumenitin-R and eumenitin-F, which are highly homologous to eumenitin (Fig. 8B).

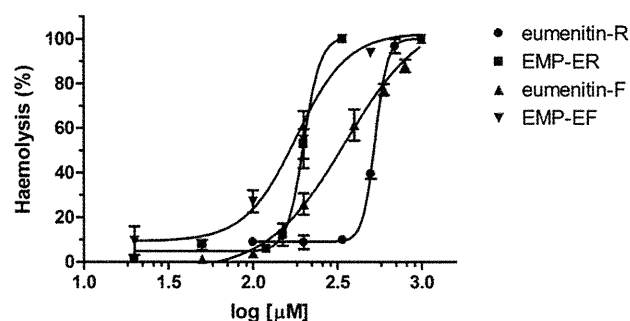


Fig. 7. The dose–response curves of the hemolytic activity of the wasp venom peptides in mouse erythrocytes show a dose-dependent relation. More hydrophilic peptides, eumenitin-R and eumenitin-F, present higher EC₅₀ values. See also Table 3.

Table 4

Effective concentration (EC₅₀) of hemolytic activity of the wasp peptides and the 95% confidence intervals (CI), in μM ($n = 4$).

Peptide	EC ₅₀ (μM)	95% CI
Eumenitin-R	530.3	512.9 to 548.3
EMP-ER	200.0	189.6 to 211.0
Eumenitin-F	353.4	251.7 to 496.3
EMP-EF	181.1	142.6 to 229.9

3.4.4. Leishmanicidal activity

The results of the leishmanicidal assay are summarized in Table 5. For comparison, eumenitin and EMP-AF were also tested. Most peptides showed an activity, but only moderately. It is noteworthy that the eumenitin series (C-terminal free) are weaker than the EMP series (C-terminal amide). This is similar to our previous results of decoralin (C-terminal free) vs. decoralin-NH₂ (C-terminal amide) (Konno et al., 2007).

4. Discussion

In the present study, we have purified four new linear cationic α -helical peptides from two species of the eumenine solitary wasps, *E. rubrofemoratus* and *E. fraterculus*, and characterized them both chemically and biologically. Of these, eumenitin-R and eumenitin-F are highly homologous to eumenitin, whereas the others, eumenine mastoparan-ER (EMP-ER) and eumenine-mastoparan-EF (EMP-EF), are similar to EMP-AF, and thus, can be classified into mastoparan peptides. These results suggested that these types of peptide are commonly and widely distributed in the eumenine wasp venoms. All these peptides and anoplin present the following common interesting physicochemical and biological features: short chain length – 10 to 15 residues long, polycationic character, they assume α -helical conformation upon contact with membrane mimetic environments, and they are antimicrobial, hemolytic and mast cell degranulators at various levels.

Conformational and pore-forming activity of these new peptides were investigated in asolectin bilayers, which due to its anionic character mimic the cytoplasmic membrane

of bacteria. This phospholipid, whose approximate composition is 23.5% phosphatidylcholine, 20% phosphatidylethanolamine, and 14% inositol phosphatides (other components are 39.5% other phospholipids, lipids and carbohydrates, and 2% triglycerides, tocopherols, sterols), holds some similarities to the lipid composition of rat mast cells; the phospholipids amount roughly to 50% of the total lipids, from these phospholipids is 30%, phosphatidylethanolamine 27%, sphingomyelin 20%, and phosphatidylserine and phosphatidylinositol are 16%. An important difference lies in that cholesterol represent around 20% of the total lipids content in rat mast cell membranes, while in asolectin sterols, it represents less than 0.3% (Strandberg and Westerberg, 1976). In relation to sterols and the general anionic character, this bilayer can also be considered a mimetic of microbial membranes. Thus the behavior of these new Eumenine peptides can be reasonably well modeled and their mechanism of action understood through the use of asolectin bilayers.

Peptides such as mastoparans adopt an amphipatic α -helical conformation in anisotropic or membrane mimetic media (Wakamatsu et al., 1992; Chuang et al., 1996; Hori et al., 2001; Sforça et al., 2004; Todokoro et al., 2006). Similarly the four peptides in our study presented circular dichroism spectra that are characteristic of helical structures with practically equivalent α -helix content, except for EMP-ER, which showed a higher helical content.

The experiments of electrical measurements in planar lipid bilayers of anionic asolectin showed that all the new peptides present a pore- or channel-like activity, in both the positive and negative voltage pulses, as previously demonstrated for eumenitin (Arcisio-Miranda et al., 2008), anoplin (dos Santos Cabrera et al., 2008) and other mastoparan peptides (Mellor and Sansom, 1990; dos Santos Cabrera et al., 2009). Channels with lower and higher conductance levels were recorded, but the latter ones were less frequent, and formed only in the presence of the non-amidated C-terminal peptides (eumenitin-R and eumenitin-F).

The channel-like activity of these peptides is similar to that observed with eumenitin in the same lipid bilayer as

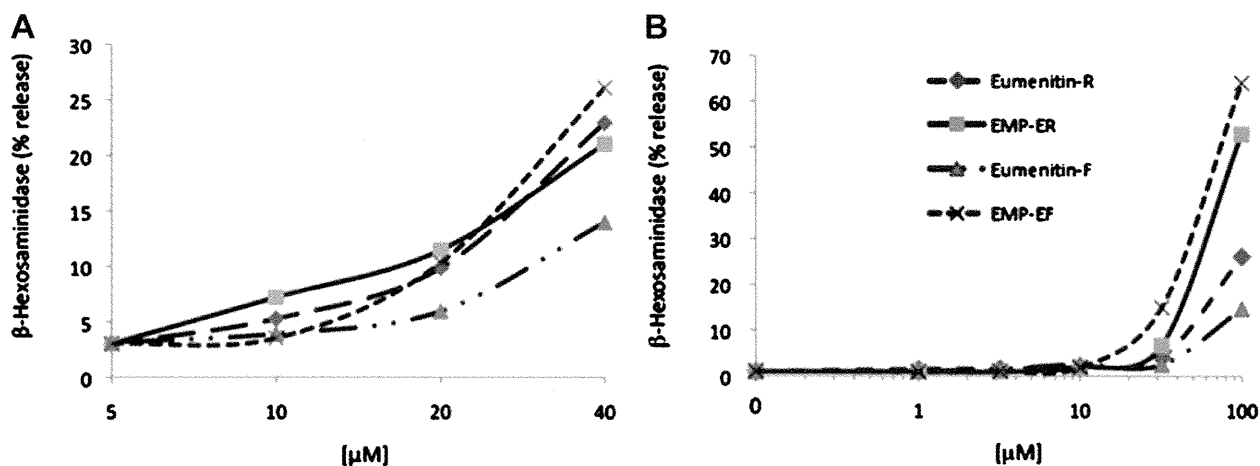


Fig. 8. The degranulation in PT18 cells (A: a connective tissue-type mast cell model) and RBL-2H3 cells (B: a mucosal-type mast cell model) measured by the β -hexosaminidase release, basal and after treatment with the peptides from the wasps *Eumenes rubrofemoratus* (eumenitin-R and EMP-ER) and *Eumenes fraterculus* (eumenitin-F and EMP-EF). Concentrations are in μM (values inside parentheses). Data represent the mean from 2–4 independent experiments.

Table 5

Leishmanicidal activity of the wasp venom peptides.

Peptide	IC ₅₀ (μM) ^a
Eumenitin	35
Eumenitin-R	>62
Eumenitin-F	52
EMP-ER	20
EMP-EF	40
EMP-AF	35
Amphotericin B ^b	<0.1

^a IC₅₀: 50% inhibitory concentration.^b Used as positive control.

could be foreseen from the high homology in their respective sequences. However, eumenitin-F channels presented strong rectification under negative voltage pulses, similarly to the mastoparan peptide HR-1 pores, whose conductances were nearly four times higher when the V_{hold} was changed to negative pulses (dos Santos Cabrera et al., 2009).

Concerning EMP-ER and EMP-EF, their pore conductance levels are equivalent to those for mastoparan HR-1, although they present a lower degree of homology, different net charges and different hydrophobicities (Fig. 2 and Table 1). These physicochemical differences could account for the double conductance levels found with EMP-ER and EMP-EF, which were not detected in HR-1 (dos Santos Cabrera et al., 2009).

Overall, the electrophysiology results confirmed the lytic activity of these new peptides. Short chain peptides, shorter than the bilayer thickness, made of bulky residues and showing pore-like activity combine characteristics that favor the toroidal pore model (Matsuzaki et al., 1996; Yang et al., 2001), by which the pore is described as a complex made of lipid molecules, predominantly, and peptide molecules that induced the bilayer destabilization by inserting into it. Models describing peptide membrane interactions have recently been determined as not reflecting static structures to which one or multiple peptide monomers contribute (Quian et al., 2008; Marsh, 2009; Leontiadou et al., 2006; Herce and Garcia, 2007). Additional experiments to describe the mechanisms of pore formation, besides the preliminary results described herein, are currently ongoing in our laboratories. Based on the bioassays performed with the synthetic peptides, their antimicrobial, leishmanicidal and cytolytic properties were determined. The leishmanicidal activity of the peptides was detected in concentrations similar or slightly higher than the antimicrobial activity, and EMP-ER presented the strongest inhibition of the *L. major* promastigotes. This activity was dependent of the C-terminal amide, in a way similar to the results with decoralin vs. decoralin-NH₂ (Konno et al., 2007). All four peptides induced mast cell degranulation in a dose-dependent manner with similar potencies. The peptides were also hemolytic against mouse erythrocytes, but in higher concentrations than those used in the antimicrobial assays. The peptides eumenitin-R and eumenitin-F showed a weak hemolytic activity, probably because of the low hydrophobicity, in a way similar to eumenitin (Konno et al., 2006) or also due to the lack of the C-terminal amide modification as in EMP-AF1 (dos Santos Cabrera et al., 2004). Furthermore, the peptides eumenitin-R and to a similar extent eumenitin-F, presented

the strongest antimicrobial activity, which could be attributed to their higher net charges (Dathe and Wieprecht, 1999; Dathe et al., 2002). All four peptides inhibited the growth of the yeast *C. albicans* at low concentrations, and again we emphasize the eumenitin-R activity.

Based on these results, eumenitin-R appears as the peptide showing higher potential as a leading compound in drug development. Like eumenitin it associates an average net charge and low hydrophobicity, which resulted in an interesting antimicrobial activity, mainly considering clinical samples, and practically devoid of undesirable effects as hemolytic and mast cell degranulating activities.

Conflict of interest

The authors declare that there are no conflicts of interest.

Acknowledgements

The authors thank Dr. Christoph Borchers, Facility Director of the University of Victoria Proteomics Centre, Canada, for the cooperation on the peptides synthesis and Prof. Dr. João Ruggiero Neto for the use of the CD equipment and the laboratory facilities. This work was supported by FAPESP – Fundação de Amparo à Pesquisa do Estado de São Paulo, Brazil (2008/00173-4), CNPq – Conselho Nacional de Desenvolvimento Científico e Tecnológico, Brazil (307457/2008-7); MPSC acknowledges the support of CNPq (477507/2008-5).

References

- Arcisio-Miranda, M., Cabrera, M.P.S., Konno, K., Rangel, M., Procopio, J., 2008. Effects of the cationic antimicrobial peptide Eumenitin from the venom of solitary wasp *Eumenes rubronotatus* in planar lipid bilayers: surface charge and pore formation activity. *Toxicon* 51, 736–745.
- Chuang, C.C., Huang, W.C., Yu, H.M., Wang, K.T., Wu, S.H., 1996. Conformation of *Vespa basalis* mastoparan-B in trifluoroethanol-containing aqueous solution. *Biochim. Biophys. Acta* 1292, 1–8.
- Dathe, M., Wieprecht, T., 1999. Structural features of helical antimicrobial peptides: their potential to modulate activity on model membranes and biological cells. *Biochim. Biophys. Acta* 1462, 71–87.
- Dathe, M., Meyer, J., Beyermann, M., Maul, B., Hoischen, C., Bienert, M., 2002. General aspects of peptide selectivity towards lipid bilayers and cell membranes studied by variation of the structural parameters of amphipathic helical model peptides. *Biochim. Biophys. Acta* 1558, 171–186.
- Eisenberg, D., Schwarz, E., Komaromy, M., Wall, R., 1984. Analysis of membrane and surface protein sequences with the hydrophobic moment plot. *J. Mol. Biol.* 179, 125–142.
- Eldefrawi, A.T., Eldefrawi, M.E., Konno, K., Mansour, N.A., Nakanishi, K., Oltz, E., Usherwood, P.N.R., 1988. Structure and synthesis of a potent glutamate receptor antagonist in wasp venom. *Proc. Natl. Acad. Sci. U S A* 85, 4910–4913.
- Fertig, N., Blick, R.H., Behrends, J.C., 2002. Whole cell patch clamp recording performed on a planar glass chip. *Biophys. J.* 82, 3056–3062.
- Herce, H., Garcia, A.E., 2007. Molecular dynamics simulations suggest a mechanism for translocation of the HIV-1 TAT peptide across lipid membranes. *Proc. Natl. Acad. Sci. U S A* 104, 20805–20810.
- Hori, Y., Demura, M., Iwadate, M., Ulrich, A.S., Niidome, T., Aoyagi, H., Asakura, T., 2001. Interaction of mastoparan with membranes studied by 1H-NMR spectroscopy in detergent micelles and by solid-state 2H-NMR and 15N-NMR spectroscopy in oriented lipid bilayers. *Eur. J. Biochem.* 268, 302–309.
- Konno, K., Hisada, M., Miwa, A., Itagaki, Y., Naoki, H., Kawai, N., Yasuhara, T., Takayama, H., 1998. Isolation and structure of

- pompilidotoxins (PMTXs), novel neurotoxins in solitary wasp venoms. *Biochem. Biophys. Res. Commun.* 250, 612–616.
- Konno, K., Hisada, M., Naoki, H., Itagaki, Y., Kawai, N., Miwa, A., Yasuhara, T., Morimoto, Y., Nakata, Y., 2000. Structure and biological activities of eumenine mastoparan-AF (EMP-AF), a novel mast cell degranulating peptide in the venom of the solitary wasp *Anterhynchium flavomarginatum micado*. *Toxicon* 38, 1505–1515.
- Konno, K., Hisada, M., Fontana, R., Lorenzi, C.C.B., Naoki, H., Itagaki, Y., Miwa, A., Kawai, N., Nakata, Y., Yasuhara, T., Ruggiero Neto, J., de Azevedo, W.F., Palma, M.S., Nakajima, T., 2001. Anoplin, a novel antimicrobial peptide from the venom of the solitary wasp *Anoplius samariensis*. *Biochim. Biophys. Acta* 1550, 70–80.
- Konno, K., Hisada, M., Naoki, H., Itagaki, Y., Fontana, R., Rangel, M., Oliveira, J.R., Cabrera, M.P.S., Ruggiero Neto, J., Hide, I., Nakata, Y., Yasuhara, T., Nakajima, T., 2006. Eumenitin, a novel antimicrobial peptide from the venom of the solitary eumenine wasp *Eumenes rubronotatus*. *Peptides* 27, 2624–2631.
- Konno, K., Rangel, R., Oliveira, J.S., Cabrera, M.P.S., Fontana, R., Hirata, I.Y., Hide, I., Nakata, Y., Mori, K., Kawano, M., Fuchino, H., Sekita, S., Ruggiero Neto, J., 2007. Decoralin, a novel linear cationic α -helical peptide from the venom of the solitary eumenine wasp *Oreumenes decoratus*. *Peptides* 28, 2320–2327.
- Kuhn-Nentwig, L., 2003. Antimicrobial and cytolytic peptides of venomous arthropods. *Cell. Mol. Life Sci.* 60, 2651–2668.
- Leontiadou, H., Mark, A.E., Marrink, S.J., 2006. Antimicrobial peptides in action. *J. Am. Chem. Soc.* 128, 12156–12161.
- Marsh, D., 2009. Orientation and peptide-lipid interactions of alamethicin incorporated in phospholipid membranes: polarized infrared and spin-label EPR spectroscopy. *Biochemistry* 48, 729–737.
- Matsuzaki, K., Murase, O., Fujii, N., Miyajima, K., 1996. An antimicrobial peptide, magainin 2, induced rapid flip-flop of phospholipids coupled with pore formation and peptide translocation. *Biochemistry* 35, 11361–11368.
- Mellor, I.R., Sansom, M.S., 1990. Ion-channel properties of mastoparan, a 14-residue peptide from wasp venom, and of MP3, a 12-residue analogue. *Proc. R. Soc. Lond. B Biol. Sci.* 239, 383–400.
- Murata, K., Shinada, T., Ohfuné, Y., Hisada, M., Yasuda, A., Naoki, H., Nakajima, T., 2009. Novel mastoparan and protonectin analogs isolated from a solitary wasp, *Orancistrocerus drewseni drewseni*. *Amino Acids* 37, 389–394.
- Ortega, E., Schneider, H., Pecht, I., 1991. Possible interactions between the Fc epsilon receptor and a novel mast cell function-associated antigen. *Int. Immunol.* 3, 333–342.
- Park, N.G., Yamato, Y., Lee, S., Sugihara, G., 1995. Interaction of mastoparan-B from venom of a hornet in Taiwan with phospholipid bilayers and its antimicrobial activity. *Biopolymers* 36, 793–801.
- Prates, M.V., Sforça, M.L., Regis, W.C.B., Leite, J.R.S.A., Silva, L.P., Pertinhez, T.A., Araújo, A.L.T., Azevedo, R.B., Spisni, A., Bloch Jr., C., 2004. The NMR-derived solution structure of a new cationic antimicrobial peptide from the skin secretion of the anuran *Hyla punctata*. *J. Biol. Chem.* 279, 13018–13026.
- Quian, S., Wang, W., Yang, L., Huang, H.W., 2008. Structure of transmembrane pore induced by bax-derived peptide: evidence for lipidic pores. *Proc. Natl. Acad. Sci. U S A* 105, 17379–17383.
- Rangel, M., Malpezzi, E.L.A., Ssusi, S.M.M., Freitas, J.C., 1997. Hemolytic activity in extracts of the diatom *Nitzschia*. *Toxicon* 35, 305–309.
- Rohl, C.A., Baldwin, R.L., 1998. Deciphering rules of helix stability in peptides. *Meth. Enzymol.* 295, 1–26.
- dos Santos Cabrera, M.P., Souza, B.M., Fontana, R., Konno, K., Palma, M.S., de Azevedo, W.F., Ruggiero Neto, J., 2004. Conformation and lytic activity of eumenine mastoparan: a new antimicrobial peptide from wasp venom. *J. Pept. Res.* 64, 95–103.
- dos Santos Cabrera, M.P., Arcisio-Miranda, M., Costa, S.T.B., Konno, K., Ruggiero Jr., Procopio, J., Ruggiero Neto, J., 2008. Study of the mechanism of action of anoplin, a helical antimicrobial decapeptide with ion channel-like activity, and the role of the amidated C-terminus. *J. Pept. Sci.* 14, 661–669.
- dos Santos Cabrera, M.P., Arcisio-Miranda, M., da Costa, L.C., de Souza, B. M., Costa, S.T.B., Palma, M.S., Ruggiero Neto, J., Procopio, J., 2009. Interactions of mast cell degranulating peptides with model membranes: a comparative biophysical study. *Arch. Biochem. Biophys.* 486, 1–11.
- Sforça, M.L., Oyama Jr., S., Canduri, F., Lorenzi, C.C.B., Pertinhez, T.A., Konno, K., Souza, B.M., Palma, M.S., Ruggiero Neto, J., de Azevedo Jr., W.F., Spisni, A., 2004. How C-terminal carboxyamidation alters the biological activity of peptides from the venom of the eumenine solitary wasp. *Biochemistry* 43, 5608–5617.
- Sondermann, M., George, M., Fertig, N., Behrends, J.C., 2006. High-resolution electrophysiology on a chip: transient dynamics of alamethicin channel formation. *Biochim. Biophys. Acta* 1758, 545–551.
- de Souza, B.M., dos Santos Cabrera, M.P., Ruggiero Neto Jr., J., Palma, M.S., 2010. Investigating the effect of different positioning of lysine residues along the peptide chain of mastoparans for their secondary structures and biological activities. *Amino Acids*. doi:10.1007/s00726-010-0481-y.
- Strandberg, K., Westerberg, S., 1976. Composition of phospholipids and phospholipid fatty acids in rat mast cells. *Mol. Cell. Biochem.* 11, 103–107.
- Takahashi, M., Fuchino, H., Satake, M., Agatsuma, Y., Sekita, S., 2004. In vitro screening of leishmanicidal activity of Myanmar timber extracts. *Biol. Pharm. Bull.* 27, 921–925.
- Todokoro, Y., Yumen, I., Fukushima, K., Kang, S.-W., Park, J.S., Kohno, T., Wakamatsu, K., Akutsu, H., Fujiwara, T., 2006. Structure of tightly membrane-bound mastoparan-X, a G-protein-activating peptide, determined by solid-state NMR. *Biophys. J.* 91, 1368–1379.
- Wakamatsu, K., Okada, A., Miyazawa, T., Ohya, M., Higashijima, T., 1992. Membrane-bound conformation of mastoparan-X, a G protein-activating peptide. *Biochemistry* 3, 5654–5660.
- Wayne, P.A., 2004. NCCLS. Performance Standards for Antimicrobial Susceptibility Testing; Fourteenth Informational Supplement, vol. 24(1). National Committee of Clinical Laboratory Standards. NCCLS document M100-S14.
- Wimley, W.C., 2010. Describing the mechanism of antimicrobial peptide action with the interfacial activity model. *ACS Chem. Biol.* 5, 905–917.
- Yamamoto, T., Arimoto, H., Kinumi, T., Oba, Y., Uemura, D., 2007. Identification of proteins from venom of the paralytic spider wasp, *Cyphononyx dorsalis*. *Insect Biochem. Mol. Biol.* 37, 278–286.
- Yang, L., Harroun, T.A., Weiss, T.M., Ding, L., Huang, H.W., 2001. Barrel-stave model or toroidal model? A case study on melittin pores. *Biophys. J.* 81, 1475–1485.
- Yasuhara, T., Mantel, P., Nakajima, T., Piek, T., 1987. Two kinins isolated from an extract of the venom reservoirs of the solitary wasp *Megascolia flavifrons*. *Toxicon* 25, 527–535.
- Yeaman, M.R., Yount, N.Y., 2003. Mechanisms of antimicrobial peptide action and resistance. *Pharmacol. Rev.* 55, 27–56.

